Modeling and Control of Reconfigurable Quadrotors Based on Model Reference Adaptive Control

Zhiping Liu *, Guoshao Chen , Shuping Xu

Posted Date: 22 March 2024

doi: 10.20944/preprints202403.1324.v1

Keywords: underactuated system; reconfigurable; multi-rotor; flight control; simulation

Article

Modeling and Control of Reconfigurable Quadrotors Based on Model Reference Adaptive Control

Zhiping Liu *, Guoshao Chen and Shuping Xu

School of Computer Science and Engineering, Xi'an Technological University, Xi'an 710021,China; leopard@xatu.edu.cn(Z.L.);chen13772482272@163.com(G.C.);563937848@qq.com(S.X.)

* Correspondence: leopard@xatu.edu.cn; Tel.: +86-13679280596

Abstract: With much more challenging scenarios encountered in engineering, traditional quadrotors couldn't accomplish all desired missions perfectly. Task-driven based reconfigurable quadrotors have more latent capacity in environment with dense obstacles and narrow corridors. The translational reconfigurable quadrotors and rotational reconfigurable quadrotors are proposed in this presentation, assumptions, mathematical models and related motion control laws are given subsequently, in order to cope with hazard missions, model reference adaptive control laws are proposed, sufficient numerical simulations demonstrate the validity of the proposed control laws.

Keywords: underactuated system; reconfigurable; multi-rotor; flight control; simulation

1. Introduction

During the past decades, the traditional multi-rotor unmanned aerial vehicles (UAVs) have been applied in the military and civil fields, such as photography, search, inspection, detection, rescue and surveillance, meanwhile the multi-rotor has been a scientific research platform to demonstrate the improvements in control theory, optimization algorithms, visual navigation and flight control, and even reinforcement learning[1–6]. Although dramatic growth of research efforts in the multi-rotor UAV has been seen recently, much more hazardous missions and challenges urgently needs to be tackled. For instance, more and more uncertain disturbances and unknown environments should be taken into consideration. In order to deal with these challenges, the research of new mechanical designs, control strategies and effective load integration, information fusions algorithms and related simulations should be performed continuously.

In reference [1], the authors present a complimentary filter to estimate the linear velocity of quadrotors in inertial frame while the UAV flies in challenging environment，besides the theoretical design and analysis, the comparisons of presented approach with other fashionable methods are also given, both theoretically and experimentally. In order to resolve the control allocation and optimization of tilting UAV, the authors in reference [2] propose a model predictive control method and then give simulation results and experimental results to verify its validity. While the reconfiguration in reference [3] is reconfigurable formation of quadrotors, agent addition, agent removal and agent replacement is the research focus, the detailed theoretical analysis and simulation results are given finally. Novel mechanical design has been the prominent tendency, in reference [4] a passive rotary joint is presented to realize morphing quadrotors and this design can reduce the dimension of the quadrotors nearly 50%, meanwhile this kind of quadrotors can travel through the narrow gap for which the ordinary quadrotors could not accomplish. Apart from the passive reconfiguration design, in reference [5] the author proposes an active reconfigurable design scheme, namely transformable UAV, and which is a new hybrid UAV and can transform its flight mode from rigid wing to rotary wing, detailed theory analysis and experimental test validate the feasibility of the proposed prototype and design ideas. Authors in reference [6] deal with the manipulation redundancy of quad-tilt rotors in conversion process and flight test, finally give the simulation and experimental test to show the validity. The motion stability and performance problem of quadrotors

 doi:10.20944/preprints202403.1324.v1

in wind were addressed in reference [7], both translational motion problem and rotational motion problem are resolved, experimental results show that the proposed scheme for dealing with the wind disturbances is reasonable and feasible. Besides the angular reconfigurations discussed above, in reference [8] a linear reconfiguration model is proposed. Because of the center of mass of the whole quadrotors varies with the position of each rotors, the authors present the detailed calculation of center of mass and inertia tensors and then give the position control and attitude control laws, and finally give the simulation and experimental test. Being different from the aforementioned reconfiguration modes, two rotors simultaneously rotate relative to the quadrotor body was presented in reference [9]. Each arm of the quadrotors has its own rotatory servo mechanism, each arm has two rotors to support lift force and moments. Systematic model is proposed and validity is proven by experimental tests. A foldable quadrotors which can squeeze and traverse a narrow gap is reported in the reference [10]，there are four independent motors to change the position of each rotor. Associated mathematical model and analysis is given, experimental test verify the superiority over the traditional configuration quadrotors in traversing narrow gap and grasping aerial objects. A self-reconfiguration mode is proposed in reference [11], and it can deal with the rotor failures during the flight using mixed integer linear programming algorithm. Reference [12] presented the reconfigurable flight control model and applied the sliding mode control method to the design of control law. In order to alleviating the effect of parasitic dynamics, asymptotic observer is proposed and finally the simulation results show the tracking and robustness of sliding mode control laws is superior to that of classic, loop-shaping methods. Author in reference [13] presents the design and control of a variable-pitch quadrotors to overcome the maneuverability limitations of the traditional quadrotors, meanwhile give the detailed analysis of the potential benefits of this kind of quadrotors and experimental tests results. A novel morphing quadrotors which can change its topological modes by rotating hinges was proposed in reference [14], and reinforcement learning is used to optimize the attitude control laws, the experimental test on a real morphing quadrotor platform was performed and results validate the excellent performance of the proposed control laws. A reconfigurable aerial robots chain was presented in reference [15], the chain can cross narrow sections, morph its shape and therefore has excellent extensibility. The systematic dynamics model of the chain was given and model predictive control laws are presented, experimental tests show that the chain can cross the narrow windows. An integrated vehicle was proposed in the reference [16], so called integrated means that it can move on the ground and can fly in the air. The detailed dynamical model and control allocation was presented, experimental tests validate the reasonability. Authors in reference [17] proposed adaptive sliding mode control laws to deal with the finite time stability of quadrotors, the simulation results show the validity of the proposed control method, obviously it's better to do experiment to test the robustness of the adaptive sliding mode control. In reference [18], for the sake of dissociating the translational motion and angular motion of traditional quadrotors, a tilt mechanism was added to the standard quadrotors configuration, and then linear quadratic regulator and model predictive control laws are derived to control the attitude and position of tilting quadrotors, numerical simulations demonstrated the validity of the mechanism and control laws. Reference [19] presents reconfigurable multicopter concept and dynamic simulation models, meanwhile analyze the relationship between the multicopter mass and power requirements, exhibits the longitudinal modes and lateral modes of different configurations. In order to address the control problems of quadrotors with unknown mass and inertia, reference [20] presents a multiple-model adaptive control architecture, control of height and yaw angle is based on linear quadratic regulator, simulation and experimental tests validate the feasibility of the proposed architecture. To deal with flight safety problems resulted from actuators failure, reference [21] choose hexarotor to address the feasibility of reconfiguration design and extend the maneuverability, outdoor experimental tests demonstrate the feasibility of reconfigurable structure under one rotor failure. Reference [22] reviews the current state of modular reconfigurable robots and associated techniques, although it’s not directly focus on the aerial vehicles, its ideas can be used to design and analyze the reconfigurable quadrotors in the future. To tackle the external disturbances of quadrotors, in reference [23] a hybrid finite-time trajectory tracking scheme was proposed, wherein the adaptive integral sliding mode

 doi:10.20944/preprints202403.1324.v1

control law was used to control the attitude subsystem and backstepping technique was deployed to control position subsystem, all the control laws are companioned with finite time disturbance observer, simulation results show that proposed control scheme has superior performance. Authors in the reference [24] presents a control system design scheme to deal with the propeller failure of quadrotors, added four mechanisms are used to enhance the controllability, subsequently the system modeling and control law are designed, simulation and experimental results show that proposed scheme can tackle the propeller failure in routine flight. In order to enlarge the flight envelope and execute much more missions, reference [25] presents a hybrid tilt-rotor configuration for traditional quadrotors, through theoretical research and simulation tests are carried out to verify the reasonability and feasibility. In order to enhance the obstacle avoiding ability, a deformable quadrotors was proposed in reference [26]. A scissor-like mechanical structure was used to realize the deformation of the quadrotor when encountering the obstacles during the flight. Extended simulation and experimental tests are conducted to verify the effectiveness of the proposed design. How to change the underactuated quadrotor to fully actuated quadrotor has been an open problem in the field of quadrotor application, a new fully actuated quadrotor was presented in reference [27], detailed control architecture was proposed and experimental tests validate the proposed design. One of the fully actuated quadrotors was presented in reference [28], it consists of upper and lower parts from the point of view of mechanism, and then robust control algorithms are developed, the simulation and experimental tests of fully actuated prototype validate the proposed scheme.

In a word, reconfigurable quadrotors have potentiality in the future applications, more scientific problems and technical problems need to be tackled, not only involve various external disturbances and uncertainties, but also optimization of mechanical configuration, control strategies and information processing, this is the motivation to do associated research presented herein.

Based on the aforementioned reconfigurable structures and associated control law designs, stability, robustness to external disturbances and quick response ability are still significant issues to be addressed. What the corresponding mathematical model is, how to design a reasonable control law to stabilize this time varying system and how to calculate the time varying adaptive control gains are main objectives.

The contributions of this paper can be listed below. 1)The mathematical model of basic translational and rotational reconfigurable quadrotors is proposed, calculation of time varying inertia parameters is given. 2)Model reference adaptive control laws are designed based on Lyapunov functions. 3)Control matrix of the reconfigurable quadrotors is given, according to the best of my knowledge, this is the first time listed in open literature. 4)The effect of time constant of reference model on control performance is considered. 5)The simulation model is constructed and simulation results validate the proposed control laws.

The reminder of this paper is organized as follows. Detailed problem formulation and reasonable assumptions are described in section II, then the kinematic model and dynamic model of the proposed reconfigurable quadrotors are proposed, meanwhile the command signals and control laws are discussed in section III, the mathematical simulation and results analysis are presented in section IV, finally the conclusions and future work recommendations are given in section V.

2. Problem Formulation

According to the recent advances in the field of modeling and control of the quadrotors, we devote to reconfigurable design of quadrotors to enhance maneuverability and ability to meet challenging mission requirements, so a new configuration was presented, in which the linear position and angular position of four rotors can be regulated by one or more motors. From the mechanical design aspect, the reconfigurable quadrotor has two layers of different height in the quadrotor body frame. For the sake of brevity, herein the detailed mechanical design and realization of the reconfigurable body are omitted.

For the reasonability of the proposed reconfigurable quadrotor and related derivation of translational dynamics and rotational dynamics, herein some assumptions are given below.

Assumption 1 The arm of the quadrotor has same size and is made of homogeneous materials.

 doi:10.20944/preprints202403.1324.v1

Assumption 2 All the motors for regulating figuration can be simplified as mass points, all the four rotors are used for generating lift force and moments.

Assumption 3 The frictions resulted from the relative linear motion elements are neglected, because of its minority.

Assumption 4 The turbulent wind and its effect is neglected, only constant wind is considered.

Assumption 5 The linear acceleration and linear velocity of the regulating rotors relative to body frame can be measured through encoders and MEMS accelerometers.

Assumption 6 The angular acceleration and angular velocity of the regulating rotors relative to body frame can be measured through encoders, and the angular velocity of the body frame can be measured by MEMS gyros, position of quadrotors can be estimated through onboard sensors.

Assumption 7 The sensors and actuators onboard the quadrotors can be seen as qualified and meet their reliability requirements.

Assumption 8 The computer chip on board the quadrotors has enough computational capability.

Assumption 9 The battery onboard the quadrotors has at least twenty minutes of flight endurance.

Herein we will focus on the mathematical model derivation of reconfigurable quadrotors, and then taking initial value, final value constraints, time delay and external disturbances into consideration to design motion control laws. Meanwhile the center of mass and inertia tensors of the changing configuration should be calculated simultaneously, it's well known that reconfigurable quadrotors is a highly nonlinear, strongly coupled, and rapidly changing system that actuated by uncertain external disturbances and certain inputs, what we want to do is to present a mathematical model and propose reasonable control strategies, and construct simulation model and give results analysis for future applications.

3. Modeling and Control Law Design

In this section, the detailed mathematical models of several reconfigurable quadrotor will be derived and then corresponding control strategies are presented.

3.1. Kinematic Model and Dynamic Model

Based on the aforementioned assumptions, the initial or traditional configuration of quadrotor is depicted in Figure 1, and the rotational configuration is depicted in Figure 2 and translational configuration is depicted in Figure 3, and the number in the center of the rotor is the serial number of rotors on the quadrotors.

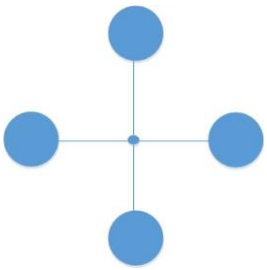

Figure 1. Traditional configuration.

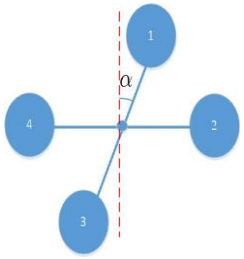

Figure 2. Rotational configuration.

 doi:10.20944/preprints202403.1324.v1

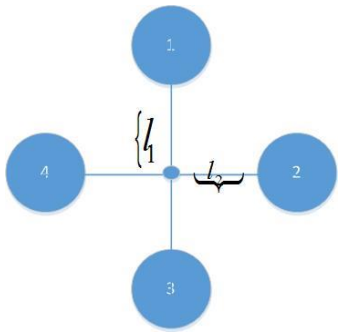

Figure 3. Translational configuration.

It's obviously can be seen that there are several combinations of above basic configurations, for the sake of brevity, herein we present the mathematical model of combination of rotational configuration and translational configuration, and this reconfiguration is described as Figure 4, the quadrotors body frame is depicted as Figure 5.

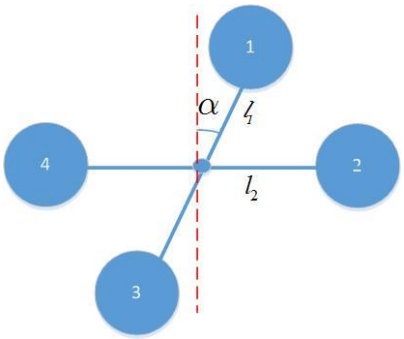

Figure 4. Combined configuration.

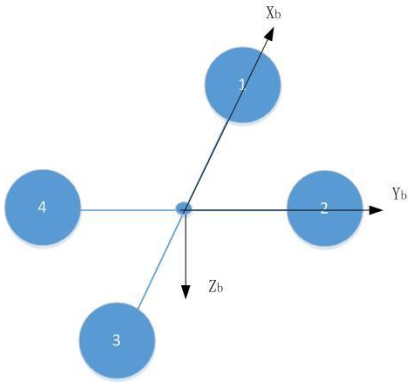

Figure 5. Body frame.

For the sake of coherence, herein all the variables used in this presentation will be described. The original length of arm is l, during the reconfigurable process its length varied with mission requirements and with a minimum value of $l_{\min} \neq 0$. The uniform linear density of the each arm is ρ_b, the vertical distance between the two arms or two layers is $2d_b$, the mass of each rotor and motor is m, each reconfigurable exciting motor is m_d, the mass of the total payload is m_p. In the original body frame, the mass of the center is at the origin of the body frame. According to corresponding calculations, it can be seen that the center of mass of the whole quadrotor doesn't change if and only if the symmetrical configuration can be hold. Therefore the mass center of the

 doi:10.20944/preprints202403.1324.v1

reconfiguration resulted by only rotation is at the origin of the body frame, while the center of the combined reconfiguration will depend on four detailed positions of the rotors and motors.

The mathematical model of reconfiguration obviously can be classified into static model and dynamics model, the static model is the model of which the reconfigurable process has been finished. While the dynamic model means that the reconfigurable process is ongoing, therefore the dynamic model has the characteristics of time variant and nonlinearity.

For the completeness of the mathematical model, herein the kinematic model and dynamic model of the pure translational reconfiguration and a simple combined reconfiguration are given below.

3.2. Model of Pure Translational Reconfiguration

We assume that the four driving motors are chosen to realize reconfiguration, each motor has relative linear velocity of $\dot{l}_i, i = 1,2,3,4$, so this scheme needs eight motors totally, four motors are used for supply necessary lift and moment, while other four exciting motors are used to realize reconfiguration.

Herein the translational dynamics model is depicted as

$$m_d + 4m_b \left(\begin{bmatrix} \dot{u} \\ \dot{v} \\ \dot{w} \end{bmatrix} + \omega \times \begin{bmatrix} u \\ v \\ w \end{bmatrix} \right) = \begin{bmatrix} 0 \\ 0 \\ -\mu_1(\omega_1^2 + \omega_2^2 + \omega_3^2 + \omega_4^2) \end{bmatrix} + R_e^b \begin{bmatrix} 0 \\ 0 \\ m_d + 4m_b \ g \end{bmatrix} + \begin{bmatrix} F_{1m} + F_{3m} \\ F_{2m} + F_{4m} \\ 0 \end{bmatrix} \quad (1)$$
$$- m_b \begin{bmatrix} \ddot{l}_1 + \ddot{l}_3 \\ \ddot{l}_2 + \ddot{l}_4 \\ 0 \end{bmatrix} - m_b \omega \times \begin{bmatrix} \dot{l}_1 + \dot{l}_3 \\ \dot{l}_2 + \dot{l}_4 \\ 0 \end{bmatrix}$$

Where u, v, w in the (1) are linear velocities of center of mass of quadrotors body with respect to the surrounding air as expressed in the body frame. ω is the angular rate of the body frame with respect to the inertial frame as expressed in the body frame. ω_i^2 is the square of the rotational rate of ith rotor. μ_1 is the coefficient of the aerodynamic lift of the rotor. g is the gravitational acceleration. R_e^b is the attitude transformation matrix which transform a vector in the earth frame to body frame. F_{im} is the locomotion force of the exciting motor, $\dot{l}_i$ is the relative translational velocity of the ith rotor with respect to the body frame, $\ddot{l}_i$ is the relative translational acceleration of ith rotor with respect to the body frame.

The rotational dynamics model is depicted as

$$J \frac{d\omega}{dt} + \dot{J}\omega + \omega \times J\omega = \begin{bmatrix} \mu_1(l_4\omega_4^2 - l_2\omega_2^2) \\ \mu_1(l_1\omega_1^2 - l_3\omega_3^2) \\ \mu_2(\omega_1^2 - \omega_2^2 + \omega_3^2 - \omega_4^2) \end{bmatrix} + m_b g R_e^b \begin{bmatrix} l_2 - l_4 \\ l_3 - l_1 \\ 0 \end{bmatrix} \quad (2)$$

Where μ_2 is the coefficient of the aerodynamic moment, the inertia tensor and its time derivative is depicted as following.

$$J = \begin{bmatrix} m_b\ l_2^2 + l_4^2\ + \frac{1}{3}\rho_b\ l_2^3 + l_4^3 & 0 & -m_b\ l_1 + l_3\ d_b \\ 0 & m_b\ l_1^2 + l_3^2\ + \frac{1}{3}\rho_b\ l_1^3 + l_3^3 & m_b\ l_2 + l_4\ d_b \\ -m_b\ l_1 + l_3\ d_b & m_b\ (+l_4\ g_b & m_b\ (^2 + l_2^2 + l_3^2 + l_4^2\ ) + \frac{1}{3}\rho_b\ (^3 + l_2^3 + l_3^3 + l_4^3\ ) \end{bmatrix} \quad (3)$$

 doi:10.20944/preprints202403.1324.v1

$$\dot{J}=\begin{bmatrix} 2m_b\ \dot{l}_2 l_2+\dot{l}_4 l_4\ +\rho_b\ \dot{l}_2 l_2^2+\dot{l}_4 l_4^2 & 0 & -m_b\ \dot{l}_1+\dot{l}_3\ d_b \\ 0 & 2m_b\ \dot{l}_1 l_1+\dot{l}_3 l_3\ +\rho_b\ \dot{l}_1 l_1^2+\dot{l}_3 l_3^2 & m_b\ \dot{l}_2+\dot{l}_4\ d_b \\ -m_b\ \left(\dot{l}_1+\dot{l}_3\right) & m_b\ \left(\dot{l}_2+\dot{l}_4\right) & 2m_b\ \left(\dot{l}_1+\dot{l}_2 l_2+\dot{l}_3 l_3+\dot{l}_4 l_4\right)+\rho_b\ \left(\dot{l}_1^2+\dot{l}_2 l_2^2+\dot{l}_3 l_3^2+\dot{l}_4 l_4^2\right) \end{bmatrix} \quad (4)$$

Corresponding to the dynamic model, the translational kinematic model is depicted as

$$\begin{bmatrix} \dot{x} \\ \dot{y} \\ \dot{z} \end{bmatrix} = R_b^e \begin{bmatrix} u \\ v \\ w \end{bmatrix} = \begin{bmatrix} c\vartheta c\psi & s\phi s\vartheta c\psi - c\phi s\psi & c\phi s\vartheta c\psi + s\phi s\psi \\ c\vartheta s\psi & s\phi s\vartheta s\psi + c\phi c\psi & c\phi s\vartheta s\psi - s\phi c\psi \\ -s\vartheta & s\phi c\vartheta & c\phi c\vartheta \end{bmatrix} \begin{bmatrix} u \\ v \\ w \end{bmatrix} \quad (5)$$

The rotational kinematic model is given below.

$$\begin{bmatrix} \dot{\phi} \\ \dot{\vartheta} \\ \dot{\psi} \end{bmatrix} = \begin{bmatrix} 1 & \sin\phi tan\vartheta & \cos\phi tan\vartheta \\ 0 & \cos\phi & -\sin\phi \\ 0 & \dfrac{\sin\phi}{\cos\vartheta} & \dfrac{\cos\phi}{\cos\vartheta} \end{bmatrix} \begin{bmatrix} p \\ q \\ r \end{bmatrix} \quad (6)$$

Where ϕ, ϑ, ψ are attitude angles of the quadrotors.

Based on the above mathematical model, and the given initial value of the state and desired locomotion force, the dynamic reconfigurable procedure can be determined through solving a set of ordinary differential equations using traditional Runge-Kutta methods.

It should be noted that although this kind of reconfiguration has eight actuators in summation, the whole system is still an underactuated one.

3.3.Model of Pure Rotational Reconfiguration

In this section, a different reconfiguration which deduced from only rotational exciter is presented.

In this configuration, we assume that the rotation rate of one arm relative to another one is $\dot{\alpha}$, for the sake of simplification, the translational dynamics of this configuration is directly given below.

$$m_d + 4m_b \left(\begin{bmatrix} \dot{u} \\ \dot{v} \\ \dot{w} \end{bmatrix} + \omega \times \begin{bmatrix} u \\ v \\ w \end{bmatrix} \right) = \begin{bmatrix} 0 \\ 0 \\ -\mu_1\ \omega_1^2 + \omega_2^2 + \omega_3^2 + \omega_4^2 \end{bmatrix} + R_e^b \begin{bmatrix} 0 \\ 0 \\ m_d + 4m_b\ g \end{bmatrix} \quad (7)$$

$$\omega = \ p, q, r + \dot{\alpha}^{\ T}$$

The rotational dynamics of this configuration is depicted as

$$J\frac{d\omega}{dt} + \dot{J}\omega + \omega \times J\omega = \begin{bmatrix} \mu_1 l\ \omega_4^2 - \omega_2^2\ + \mu_1 l\ \omega_1^2 - \omega_3^2\ \sin\alpha \\ \mu_1 l\ \omega_3^2 - \omega_1^2\ \cos\alpha \\ \mu_2\ \omega_1^2 - \omega_2^2 + \omega_3^2 - \omega_4^2 \end{bmatrix} + \begin{bmatrix} 0 \\ 0 \\ M_\alpha \end{bmatrix} \quad (8)$$

The detailed inertia matrix and its derivative with respect to time are depicted as below.

 doi:10.20944/preprints202403.1324.v1

$$J=\begin{bmatrix} 2m_b l^2\ 1+\sin^2\alpha\ +\frac{2}{3}\rho_b l^3\ 1+\sin^2\alpha & 2m_b l^2\cos\alpha\sin\alpha+\frac{2}{3}\rho_b l^3\cos\alpha\sin\alpha & 0 \\ 2m_b l^2\cos\alpha\sin\alpha+\frac{2}{3}\rho_b l^3\cos\alpha\sin\alpha & 2m_b l^2\cos^2\alpha+\frac{2}{3}\rho_b l^3\cos^2\alpha & 0 \\ 0 & 0 & 4m_b l^2+\frac{4}{3}\rho_b l^3 \end{bmatrix} \quad (9)$$

$$\dot{J}=\begin{bmatrix} 2l^2\dot{\alpha}\left(m_b+\frac{\rho_b l}{3}\right)\sin 2\alpha & 2l^2\dot{\alpha}\left(m_b+\frac{\rho_b l}{3}\right)\cos 2\alpha & 0 \\ 2l^2\dot{\alpha}\left(m_b+\frac{\rho_b l}{3}\right)\cos 2\alpha & -2l^2\dot{\alpha}\left(m_b+\frac{\rho_b l}{3}\right)\sin 2\alpha & 0 \\ 0 & 0 & 0 \end{bmatrix}$$

Where M_α is the active moment exerting on the arm 1-3 by exciting motor.

It should be noted that this configuration is deduced from traditional configuration only by one arm rotating relative to another arm.

No matter how the dynamics models vary, the kinematic model in this configuration is the same as that of described by equation (5) and (6).

3.4. Model of Translational Plus Rotational Reconfiguration

In this reconfiguration model, the translational movement of rotors and rotational movements of rotors are simultaneously taken into consideration. In this scenario, the center of mass of the whole system changes with time, meanwhile the inertia of the system around the center of the mass also varies with configuration. It's clear that this kind of configuration is complicated and is difficult to control because of the strong nonlinearity, coupling effects and time variant character.

Inspired by the work of [14], herein we give the calculation formula of the center of mass and inertia of the whole system below.

$$r_{UAV}=\frac{\sum_{i=1}^{4} m_i r_i+\sum_{i=1}^{4} m_{armi} r_{armi}}{m_{UAV}} \quad (10)$$

Where m_{UAV} is the total mass of the UAV system, m_i is the mass of the ith rotor and connected motor, m_{armi} is the mass of the ith arm of the UAV system, r_i is the displacement vector of the ith rotor in the normal initialized body frame, r_{armi} is the displacement vector of the ith arm in the normal initialized body frame. when the real center of mass of the UAV configuration has been calculated, the inertia moment of the UAV configuration based on the new center of mass can be calculated using parallel axis theorem as described in the reference [14].

For the convenient of simulation, the corresponding relationship of lift and moment with rotor speed is given below.

$$\begin{bmatrix} \omega_1^2 \\ \omega_2^2 \\ \omega_3^2 \\ \omega_4^2 \end{bmatrix}=\begin{bmatrix} \frac{l_3}{2b(l_1+l_3)} & 0 & \frac{1}{b(l_1+l_3)\cos\alpha} & \frac{l_3}{2d(l_1+l_3)} \\ \frac{l_4}{2b(l_2+l_4)} & \frac{-1}{b(l_2+l_4)} & \frac{-\sin\alpha}{b(l_2+l_4)\cos\alpha} & \frac{l_4}{2d(l_2+l_4)} \\ \frac{l_1}{2b(l_1+l_3)} & 0 & \frac{-1}{b(l_1+l_3)\cos\alpha} & \frac{l_1}{2d(l_1+l_3)} \\ \frac{l_2}{2b(l_2+l_4)} & \frac{1}{b(l_2+l_4)} & \frac{\sin\alpha}{b(l_2+l_4)\cos\alpha} & \frac{-l_2}{2d(l_2+l_4)} \end{bmatrix}\begin{bmatrix} F \\ M_x \\ M_y \\ M_z \end{bmatrix} \quad (11)$$

Where F is the lift, $M_i, i=x,y,z$ is the moment acted on the quadrotors body, this equation is so called control matrix.

 doi:10.20944/preprints202403.1324.v1

In this representation, the parameters of the researched UAV system are given below in Table 1.

Table 1. Parameters and values of the UAV system.

Physical parameter	Value
Mass of motor on the rotor	60g
Mass of driving motor	80g
Length of arm	40cm
Displacement of arm(max)	20cm
Mass of arm	30g
Mass of battery	400g
Mass of ECS	25g
Mass of payload	250g

Remark 1.The command signals in this presentation include position command signal, velocity commands, linear acceleration commands, attitude commands, angular rate commands and angular acceleration commands. All these commands are generated through command signals generator, the generated procedure is omitted herein for the sake of brevity, the detailed formulations will be given in the simulation section. The detailed design procedure of command signals can be found in reference[3,13].

3.5. Model Reference Adaptive Control Law Design

Because of the complexity of the plant itself and uncertainties of the environmental disturbances, we choose the model reference adaptive control as the method for designing the body rate tracking controllers. It should be noted that the translational controllers are designed using proportional-integral-differential method.

The complete control block diagram can be expressed as follows.

Inspired by the reference [29,30], the aforementioned models of the reconfigurable quadrotors can be depicted as follows

$$\begin{aligned} \dot{x}_p &= A_p x_p + B_p u_p \\ x_p &= \left[p, q, r\right]^T \end{aligned} \tag{12}$$

The reference model is depicted as

$$\dot{x}_m = A_m x_m + B_m r \tag{13}$$

Figure 6. reveals the idea of the model reference adaptive control, so in the equation (11) and (12), there are control inputs for plant and command signal for the reference model. It should be noted that systematic matrix and control matrix in the equation (12) and (13) all have reasonable dimensions.

 doi:10.20944/preprints202403.1324.v1

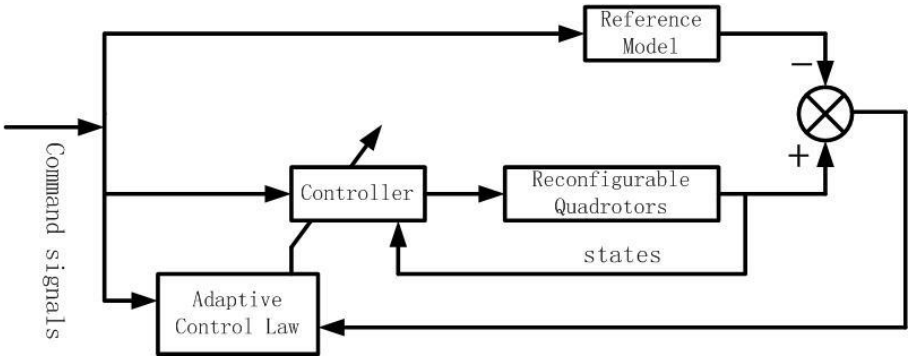

Figure 6. Adaptive Control Block.

For the sake of conveniently using the MRAC to design the body rate tracking law and attitude tracking law, the original dynamical equation (2) and (8) are rewritten as following.

$$\begin{aligned}&\dot{\omega} = A\left(\alpha, l, \dot{\alpha}, \dot{l}\right)\omega + C\left(\alpha, l\right)M + B\left(\alpha, l\right) f\left(\omega\right) + C\left(\alpha, l\right)d \\ &A\left(\alpha, l, \dot{\alpha}, \dot{l}\right) = \left[J\left(\alpha, l\right)\right]^{-1} \dot{J}\left(\alpha, l, \dot{\alpha}, \dot{l}\right) \\ &B\left(\alpha, l\right) f\left(\omega\right) = \left[J\left(\alpha, l\right)\right]^{-1}\left[\omega \times J\left(\alpha, l\right)\omega\right] \quad C\left(\alpha, l\right) = \left[J\left(\alpha, l\right)\right]^{-1}\end{aligned} \tag{14}$$

where d is external disturbances and M is command moment.

In order to derivate the control laws conveniently, we define

$$e(t) = x_p(t) - x_m(t) \tag{15}$$

It should be noted herein that $x_p(t)$ and $x_m(t)$ are not consistent with detailed translational or rotational movement variables. We suppose that the control input is of following form

$$u(t) = \Theta_x(t)x_p(t) + \Theta_r(t)r(t) \tag{16}$$

Then can get

$$\dot{x}_p(t) = \left[A_p + B_p\Theta_x(t)\right]x_p(t) + B_p\Theta_r(t)r(t) \tag{17}$$

Up to now, because of the identity of the equation (11) and equation (14), we can get desired gain matrices depicted as follows.

$$\begin{aligned}&A_p + B_p\Theta_x(t) = A_m \Rightarrow \Theta^*{}_x(t) = \left[B_p^T B_p\right]^{-1} B_p^T\left[A_m - A_p\right] \\ &B_p\Theta_r(t) = B_m \Rightarrow \Theta^*{}_r(t) = \left[B_p^T B_p\right]^{-1} B_p^T B_m\end{aligned} \tag{18}$$

As expressed in the equation (17), we consider the non square matrix formulations of the control matrix of the plant, meanwhile the error between the real state of the plant and the state from reference model vary with time, so we define the error of the gain matrices as

$$\begin{aligned}\tilde{\Theta}_x(t) &= \Theta_x(t) - \Theta^*{}_x(t) \\ \tilde{\Theta}_r(t) &= \Theta_r(t) - \Theta^*{}_r(t)\end{aligned} \tag{19}$$

Based on the above descriptions, in order to evaluate the convergence of the state error, we choose the Lyapunov function as following.

$$\begin{aligned}&V\left[e(t), \tilde{\Theta}_x(t), \tilde{\Theta}_r(t)\right] \\ &= \frac{1}{2}e^T(t)Pe(t) + Tr\left[\tilde{\Theta}_x^T(t)\Gamma_x\tilde{\Theta}_x(t)\right] + Tr\left[\tilde{\Theta}_r^T(t)\Gamma_r\tilde{\Theta}_r(t)\right]\end{aligned} \tag{20}$$

All the weight matrices in the equation (19) are supposed to be symmetric and positive definite. According to equation (19), we get

 doi:10.20944/preprints202403.1324.v1

$$\begin{aligned}&\dot{V}\left[e(t),\tilde{\Theta}_x(t),\tilde{\Theta}_r(t)\right]\\&=\frac{1}{2}\left[\dot{e}^T(t)Pe(t)+e^T(t)P\dot{e}(t)\right]+\frac{1}{2}Tr\left[\dot{\tilde{\Theta}}_x^T(t)\Gamma_x\tilde{\Theta}_x(t)+\tilde{\Theta}_x^T(t)\Gamma_x\dot{\tilde{\Theta}}_x(t)\right]\\&+\frac{1}{2}Tr\left[\dot{\tilde{\Theta}}_r^T(t)\Gamma_r\tilde{\Theta}_r(t)+\tilde{\Theta}_r^T(t)\Gamma_r\dot{\tilde{\Theta}}_r(t)\right]\end{aligned}\tag{21}$$

According to the equation (13), we have

$$\dot{e}(t)=A_m e(t)+\left[A_p+B_p\Theta_x(t)-A_m\right]x_p(t)+\left[B_p\Theta_r(t)-B_m\right]r(t)\tag{22}$$

Substituting the equation (22) in to equation (21), we have

$$\begin{aligned}&\dot{V}\left[e(t),\tilde{\Theta}_x(t),\tilde{\Theta}_r(t)\right]\\&=\frac{1}{2}e^T(t)\left[A_m^TP+PA_m\right]e(t)+\frac{1}{2}\left[x_p^T(t)\tilde{\Theta}_x^T(t)B_p^TPe(t)+e^T(t)PB_p\tilde{\Theta}_x(t)x_p(t)\right]\\&+\frac{1}{2}\left[r^T(t)\tilde{\Theta}_r^T(t)B_p^TPe(t)+e^T(t)PB_p\tilde{\Theta}_r(t)r(t)\right]+\frac{1}{2}Tr\left[\dot{\tilde{\Theta}}_x^T(t)\Gamma_x\tilde{\Theta}_x(t)+\tilde{\Theta}_x^T(t)\Gamma_x\dot{\tilde{\Theta}}_x(t)\right]\\&+\frac{1}{2}Tr\left[\dot{\tilde{\Theta}}_r^T(t)\Gamma_r\tilde{\Theta}_r(t)+\tilde{\Theta}_r^T(t)\Gamma_r\dot{\tilde{\Theta}}_r(t)\right]\end{aligned}\tag{23}$$

According to the equation (2), if the following equations are valid,

$$\begin{aligned}&A_m^TP+PA_m=-Q\\&\dot{\Theta}_x=-\Gamma_x^{-1}e^T(t)PB_px_p(t)\\&\dot{\Theta}_r=-\Gamma_r^{-1}e^T(t)PB_pr(t)\end{aligned}\tag{24}$$

Then the negative definiteness of the Lyapunov function can be assured.

$$\dot{V}\left[e(t),\tilde{\Theta}_x(t),\tilde{\Theta}_r(t)\right]=-e^T(t)Qe(t)<0\tag{25}$$

Meanwhile the gain matrices of the adaptive control strategy can be derived from the equation (23). The equations(11)-(25) are general formula to derive the adaptive control laws, in the preceding simulation, especially the body rate tracking section, the reference adaptive control laws will be derived based on following description.

The Lyapunov function is chosen as

$$V=\frac{1}{2}e^TPe+\frac{1}{2}Tr\left[\tilde{\Theta}_x^T\Gamma_1^{-1}\tilde{\Theta}_x\right]+\frac{1}{2}Tr\left[\tilde{\Theta}_r^T\Gamma_2^{-1}\tilde{\Theta}_r\right]+\frac{1}{2}Tr\left[\tilde{\Theta}_f^T\Gamma_3^{-1}\tilde{\Theta}_f\right]+\frac{1}{2}Tr\left[\tilde{\Theta}_d^T\Gamma_4^{-1}\tilde{\Theta}_d\right]\tag{26}$$

Herein the external disturbance and systematic error are considered, based on this candidate Lyapunov function, the gain matrices differential equations can be got as follow.

$$\begin{aligned}&\dot{\tilde{\Theta}}_x=-\Gamma_1C_p^TPex_p^T\qquad&&\dot{\tilde{\Theta}}_r=-\Gamma_2C_p^TPer_c^T\\&\dot{\tilde{\Theta}}_f=-\Gamma_3C_p^TPef^T\left(x_p\right)\qquad&&\dot{\tilde{\Theta}}_d=-\Gamma_4C_p^TPed^T\end{aligned}\tag{27}$$

Where $\Gamma_i, i=1,2,3,4$ denotes the positive and symmetric constant matrix.

As shown in Figure 7, the left one labeled as A is a sequential flow chart, while the right one labeled as B is a parallel flow chart, their difference only reveals the different realization of control strategies.

From the point of view of control and information processing, the detailed simulation flow chart based on MRAC is given in Figure 8. In the initialization section, waypoints and corresponding velocities, accelerations and even jerk and snap should be determined, flight duration also should be given to calculate the desired trajectory iteratively. For the sake of verifying the control laws, the time duration of reconfiguration based on normal configuration is less than 1 second. Based on this assumption, the detailed center of mass of the quadotor can be calculated and corresponding inertia of the body can be determined. In the simulation procedure, the position, attitude and velocity of the

 doi:10.20944/preprints202403.1324.v1

quadrotor can be feedback to control law design modular, this is consistent with the practical flight conditions because of the use of MEMS IMU and other onboard sensors, such as barometers and magnetometer, these sensors can be integrated to provide flight data simultaneously.

The detailed procedure of desired trajectory calculation is omitted here for the sake of brevity, interested readers can be referred to associated references.

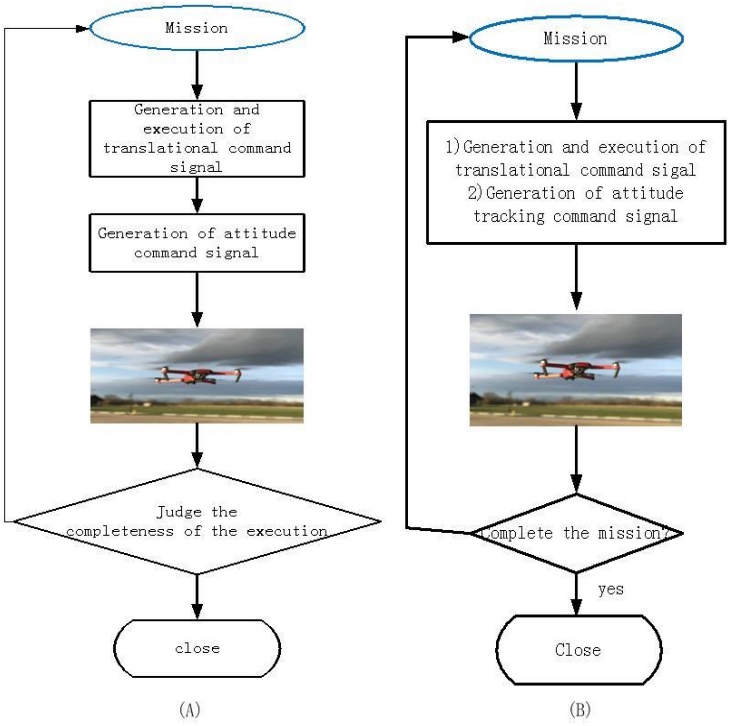

Figure 7. Control Flow Chart.

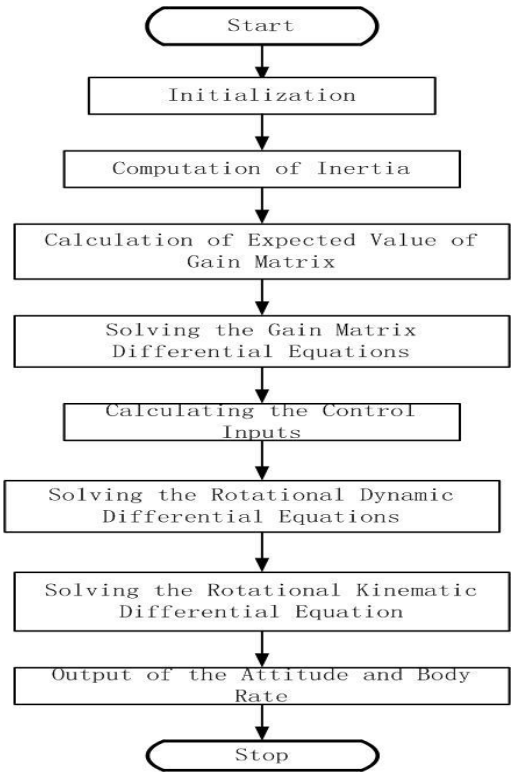

Figure 8. Simulation Flow Chart Based on MRAC.

4. Simulation and Analysis

 doi:10.20944/preprints202403.1324.v1

4.1. Initialization of simulation

In order to evaluate the proposed adaptive control method, in this section the detailed value of parameters associated with non-reconfiguration will be given in Table 2, and varying inertia value associated with reconfiguration will be calculated based on aforementioned formulas. Apart from the initial values of the inertia, the initial position, velocity and attitude of the quadrotors will also be given in this section.

In addition to the above parameters and initial conditions, the command signals to be tracked should be given in the follow sections. Because of the different scenarios have different tracking parameters, the detailed command signals herein only describe the translational command signals, associated roll angle command signal and pitch angle command signal are derived from the translational constraints.

It also should be noted that the command trajectory is designed based on the predefined waypoints and its corresponding initial velocities and accelerations, and jerk and snap can also be get through the time polynomials of the command trajectory.

Meanwhile the reference model in Figure 6 are also given below.

$$\dot{x}_M = \begin{bmatrix} \dot{p} \\ \dot{q} \\ \dot{r} \end{bmatrix}_M = daig\left[\frac{-1}{T_p}, \frac{-1}{T_q}, \frac{-1}{T_r}\right]\left(\begin{bmatrix} p \\ q \\ r \end{bmatrix}_M - \begin{bmatrix} p \\ q \\ r \end{bmatrix}_{cmd}\right) \tag{28}$$

$$\dot{x}_M = A_M x_M + B_M r$$

Where the subscript M means the measured value and subscript cmd means the command value, T is the chosen time constant of the plant.

Table 2. Necessary parameters of Quadrotors with non-reconfiguration.

Parameter	Value
I_{xx}	$0.040\, kgm^2$
I_{xy}	$0.005\, kgm^2$
I_{xz}	$0.005\, kgm^2$
I_{yy}	$0.040\, kgm^2$
I_{yz}	0
I_{zz}	$0.082\, kgm^2$

Associated parameters in this section are given below.

$$T_p = T_q = T_r = 0.006 \qquad k_{p\phi} = k_{p\vartheta} = k_{p\psi} = 1.0 \qquad k_{i\phi} = k_{i\vartheta} = k_{i\psi} = 0.5$$

$$\Gamma_1 = \begin{bmatrix} 10 & 9 & 8 \\ 9 & 10 & 7 \\ 8 & 7 & 10 \end{bmatrix} \quad \Gamma_2 = \begin{bmatrix} 12 & 9 & 8 \\ 9 & 12 & 7 \\ 8 & 7 & 12 \end{bmatrix} \quad \Gamma_3 = \begin{bmatrix} 12 & 8 & 7 \\ 8 & 12 & 6 \\ 7 & 6 & 12 \end{bmatrix} \quad \Gamma_4 = \begin{bmatrix} 11 & 8 & 7 \\ 8 & 11 & 6 \\ 7 & 6 & 11 \end{bmatrix} \tag{29}$$

Where $\Gamma_i, i = 1,2,3,4$ are chosen parameters to calculate the desired control gains and $k_{ij}, i = p, i; j = \phi, \vartheta, \psi$ are attitude control gains.

It should be noted that only the body rate command signal is presented, because of the under-actuated characteristics, the linear motion control should be achieved through angular motion control, so the detailed position command signals and velocity command signals are all omitted herein.

 doi:10.20944/preprints202403.1324.v1

The detailed mathematical simulation architecture is constructed based on MATLAB/Simulink, the whole simulation frame includes three blocks, the first block simulates the command signals and external disturbances, the second block simulates the detailed mathematical models, cases with sensor errors and without sensor errors are all taken into consideration. The third block constructs the adaptive control laws and sliding mode control laws.

In the simulation procedure, in order to evaluate the control laws equally, the sensor errors added to the measured signals are zero mean value gauss white noise with standard deviation one. All the external disturbances acting on the quadrotors are chosen as band limited white noise added with sinusoid whose amplitude is less than 0.5, the performance of the control law can be obviously distinguished through the desired actuator power and control gain.

4.2. Simulation based on MRAC

Herein the reconfigurable quadrotors means the four rotors can translate or rotate relative to the body frame, so the adaptive control law will be applied to translational reconfiguration and rotational reconfiguration.

The simulation scenario depicted in this section are used for verifying the feasibility of the MRAC, and translational reconfiguration and rotational reconfiguration take place simultaneously within 1.5 seconds, the translate velocity of rotor is less than 0.05 m/s, rotational velocity of rotor is less than 0.1 rad/s, the translate acceleration of rotor is less than 0.02 m/s^2 and rotational acceleration is less than 0.01 rad/s^2, The trajectory is smooth and with initial position $(0m, 0m, 0m)$ and final position $(5m, 5m, 4m)$ in the Earth frame, the corresponding initial attitude, initial linear velocity and angular velocity, and initial linear acceleration and angular acceleration , and final value of these parameters are omitted herein, meanwhile the final conditions are also omitted. The flight duration is 1--15 seconds, external force disturbance and external moment disturbances are chosen as constant value plus stochastic terms, extensive simulations have been conducted, the absolute value of external force is less than 1N and absolute value of external moment is less than 0.5Nm, within only partial simulation results of translational reconfiguration plus rotational reconfiguration are shown in the following section.

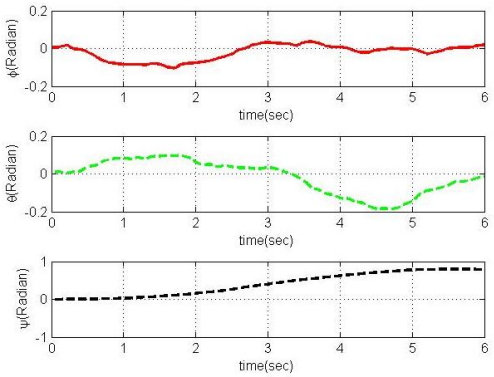

Figure 9. Attitude.

Preprints.org (www.preprints.org) | NOT PEER-REVIEWED | Posted: 22 March 2024 doi:10.20944/preprints202403.1324.v1

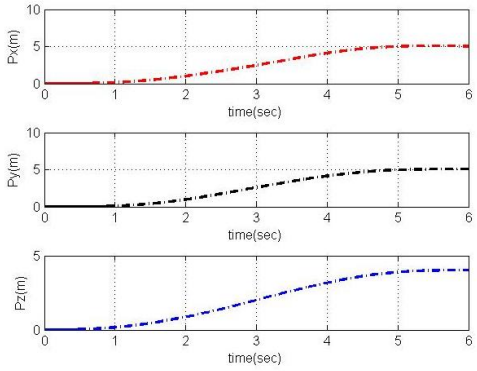

Figure 10. Position.

It can be seen that final yaw angle is nearly 0.95 radian, this value is nearly the desired final yaw angle and the position error is less than 5 centimeters. The body rate of the quadrotor and lift force is depicted in the Figure 11, and rotational speeds of four rotors are depicted in the Figure 12, the upper limit of the rotor is 900 rad/s.

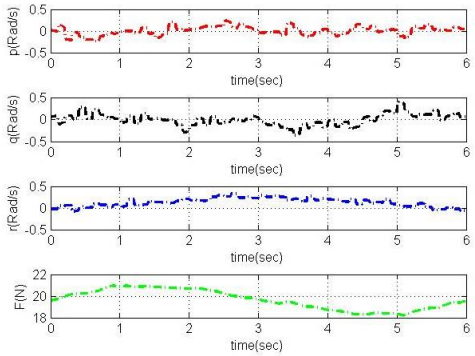

Figure 11. Body Rate and lift

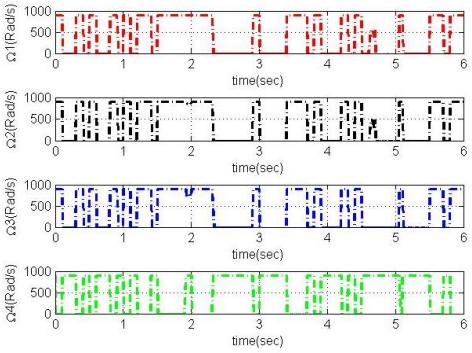

Figure 12. Speed of Rotor

The adaptive matrix gains varying with time can be shown as following.

 doi:10.20944/preprints202403.1324.v1

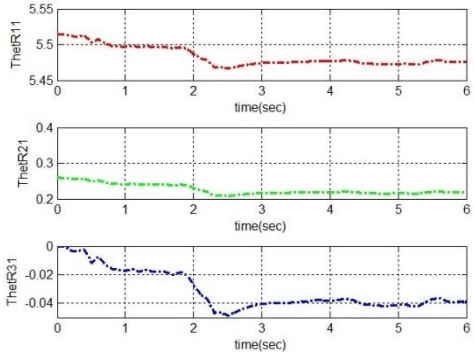

Figure 13. First column of Θ_R

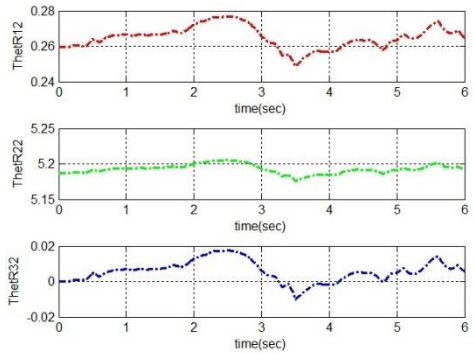

Figure 14. Second column of Θ_R

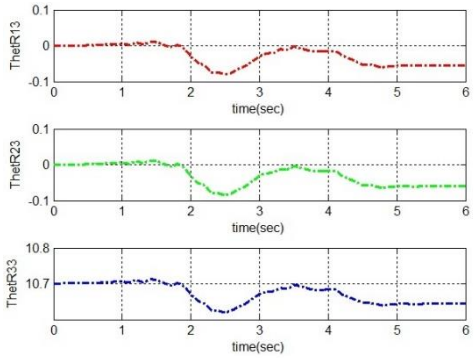

Figure 15. Third column of Θ_R

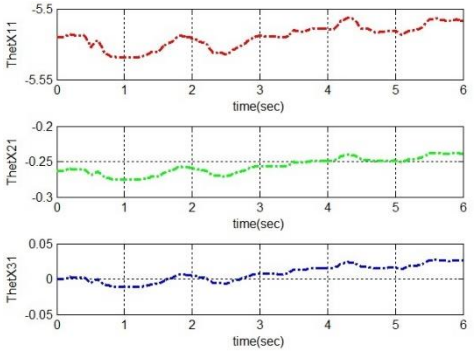

Figure 16. First column of Θ_X

Preprints.org (www.preprints.org) | NOT PEER-REVIEWED | Posted: 22 March 2024 doi:10.20944/preprints202403.1324.v1

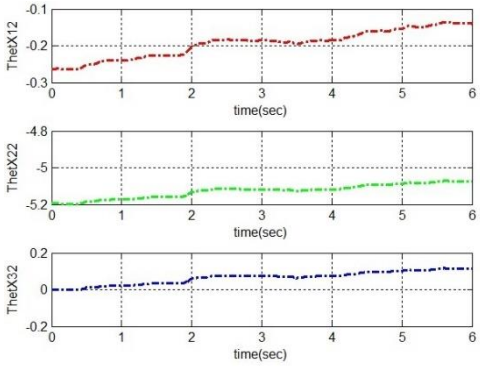

Figure 17. Second column of Θ_X

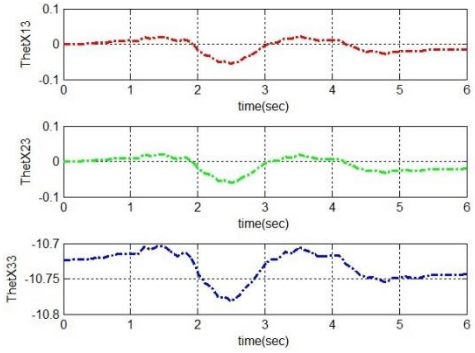

Figure 18. Third column of Θ_X

Where Θ_R is the reference signal feedback gain and Θ_X is the state feedback gain, it can be seen that the main elements are all the diagnoal ones and this is consistent with the design procedure.

It should be noted that the simulation results of Θ_f and Θ_d varying with time is omitted herein for the sake of brevity.

Although only partial flight parameters are visualized, the similarity of the associated flight parameters assured and the online calculation of ordinary differential equations can be realized through simplified algorithms.

4.3 Simulation result

Table 3 shows the qualitative results of simulation described in this section, the second column is the maximum of the flight parameters, such as attitude error and position error, while the third column is the chosen time constant of reference model, the fourth column is the value range of external forces and the fifth column is the value range of the external moments.

Table 3. Statistical simulation results.

Parameter	$\lvert\max\rvert$	$T_m(ms)$	$dF(N)$	$dM\,(Nm)$
x_e	0.2m	2~6	-0.5~1.0	-0.5~0.5
y_e	0.2m	2~6	-0.5~1.0	-0.5~0.5
z_e	0.2m	2~6	-0.5~1.0	-0.5~0.5
ϕ_e	0.1rad	2~6	-0.5~1.0	-0.5~0.5
ϑ_e	0.15rad	2~6	-0.5~1.0	-0.5~0.5

 doi:10.20944/preprints202403.1324.v1

ψ_e	0.2rad	2~6	-0.5~1.0	-0.5~0.5

Based on numerous conducted simulations, simulation results can be drawn as follows. 1) Given the same initial conditions and final conditions, the position errors and attitude errors from the MARC are within the error budget. 2) The MRAC control laws can be implemented onboard at the cost of more computational burden. 3) The choice of time constant of reference model is very important to determine the completeness of the simulation. 4) The time delay of the control vectors is a key factor to be chosen, in this presentation, this value should be less than 7 millisecond, and otherwise the simulation result will diverge rapidly. 5) MRAC control law has good dynamic performance and strong robustness with respect to external disturbances.

5. Conclusions

In this paper, the mathematical model of translational reconfiguration and rotational reconfiguration of traditional quadrotors was presented, associated assumptions about reconfigurable quadrotors were also given, then the control laws were designed using model reference adaptive control theory based on Lyapunov stability theory, simulation was performed through numerical calculation, the simulation results verify the feasibility of the proposed control laws and reveal the important effect of time delay on the stability of the motion control system, meanwhile the dependence of stability of motion control on the time constant of reference system was explicitly revealed.

In the future, the sensitivity analysis of translational velocity, rotational velocity, translational acceleration and rotational acceleration on the performance of motion control should be performed, and this is the foundation when the proposed control laws are applied to the practical engineering.

Author Contributions: Conceptualization, Z.L. and G.C.; methodology, Z.L.; software, G.C. and S.X.; validation, Z.L., G.C. and S.X.; formal analysis, Z.L. and G.C.; investigation, G.C.; resources, Z.L.; data curation, G.C.; writing—original draft preparation, Z.L.; writing—review and editing, Z.L. and G.C.; visualization, G.C. and S.X.; project administration, Z.L.; funding acquisition,Z.L.

Funding: This research was funded by the key projects of the Shaanxi Provincial Department of Science and Technology (Grant No. 2022GY-239).

Data Availability Statement: All data used during the study appear in the submitted article.

Conflicts of Interest: T All the authors declare that they have no known competing financial interests or personal relationships that could appear to influence the work reported in this paper.

References

1. M. Bangura, X. Hou, G. Allibert, R. Mahony, and N. Michael, Supervisory Control of Multirotor Vehicles in Challenging Conditions Using Inertial Measurements, IEEE Transactions on Robotics, 2018, 34(6): 1490–1501.
2. L. Bauersfeld, L. Spannagl, G. Ducard, and C. Onder, MPC Flight Control for a Tilt-Rotor VTOL Aircraft, IEEE Transactions on Aerospace and Electronic Systems, 2021, 57(4): 2395–2409.
3. A. V. Borkar, S. Hangal, H. Arya, A. Sinha, and L. Vachhani, Reconfigurable Formations of Quadrotors on Lissajous Curves for Surveillance Applications, European Journal of Control, 2020, 56: 274–288.
4. N. Bucki and M. W. Mueller, Design and Control of a Passively Morphing Quadcopter, 2019 IEEE International Conference on Robotics and Automation, Montreal, Canada, May 20-24, 2019.
5. R. R. D'Sa, Design of a Transformable Unmanned Aerial Vehicle, PhD thesis of University of Minnesota, 2020.
6. Y. Chen, Z. Wang, Z. Lyu, J. Li, Y. Yang, and Y. Li, Research on Manipulation Strategy and Flight Test of the Quad Tilt Rotor in Conversion Process, IEEE Access, 2021, 9: 40286–40307.
7. W. Craig, D. Yeo, and D. A. Paley, Geometric Attitude and Position Control of a Quadrotor in Wind, Journal of Guidance, Control and Dynamics, 2020, 43(5): 870–883.
8. M. D. Dehkordi and M. Danesh, Positionable Rotor Quadrotor: Dynamic Modeling and Adaptive Finite-Time Sliding-Mode Controller Design, Journal of Guidance, Control and Dynamics, 2022, 45(3):424–433.

9. C. Ding and L. Lu, A Tilting-Rotor Unmanned Aerial Vehicle for Enhanced Aerial Locomotion and Manipulation Capabilities: Design, Control, and Applications, IEEE/ASME Transactions on Mechatronics, 2021, 26(4): 2237–2248.
10. D. Falanga, K. Kleber, S. Mintchev, D. Floreano, and D. Scaramuzza, The Foldable Drone: A Morphing Quadrotor That Can Squeeze and Fly, IEEE Robotics and Automation Letters, 2019, 4(2): 209–216.
11. N. Gandhi, D. Saldana, V. Kumar, and L. T. X. Phan, Self-Reconfiguration in Response to Faults in Modular Aerial Systems, IEEE Robotics and Automation Letters, 2020, 5(2): 2522–2529.
12. R. A. Hess and S. R. Wells, Sliding Mode Control Applied to Reconfigurable Flight Control Design, Journal of Guidance, Control and Dynamics, 2003, 26(3): 452–462.
13. M. J. Cutler, Design and Control of an Autonomous Variable-Pitch Quadrotor Helicopter, Master's thesis of Massachusetts Institute of Technology, 2012.
14. D. Hu, Z. Pei, J. Shi, and Z. Tang, Design, Modeling and Control of a Novel Morphing Quadrotor, IEEE Robotics and Automation Letters, 2021, 6(4): 8013–8020.
15. M. Kulkarni, H. Nguyen, and K. Alexis, The Reconfigurable Aerial Robotic Chain: Shape and Motion Planning, IFAC-PaperOnline, 2020, 53(3): 9295–9302.
16. B. Li, L. Ma, D. Wang, and Y. Sun, Driving and Tilt-Hovering – An Agile and Maneuverable Aerial Vehicle with Tiltable rotors, IET Cyber-Systems and Robotics, 2021, 3(2): 103–115.
17. O. Mofid and S. Mobayen, Adaptive Sliding Mode Control for Finite-Time Stability of Quad-Rotor UAVs with Parametric Uncertainties, ISA Transactions, 2018,72: 1–14.
18. F. M. M. Marques, P. A. Q. de Assis, and R. M. F. Neto, Position Tracking of a Tilt-Rotor Quad-copter with Small Attitude Variation Using Model Predictive Control, AIAA Aviation Forum, June 15-19, 2020.
19. R. Niemiec, F. Gandhi, and R. Singh, Control and Performance of a Reconfigurable Multicopter, Journal of Aircraft, 2018, 55(5): 1855–1866.
20. P. Outeiro, C. Cardeira, and P. Oliveira, Multiple-Model Adaptive Control Architecture for a Quadrotor with Constant Unknown Mass and Inertia, Aerospace Science and Technology, 2021, 117: 106899-106912.
21. C. D. Pose, J. I. Giribet, and I. Mas, Fault Tolerance Analysis for a Class of Reconfigurable Aerial Hexarotor Vehicles, IEEE/ASME Transactions on Mechatronics, 2020, 25(4): 1851–1858.
22. J. Seo, J. Paik, and M. Yim, Modular Reconfigurable Robotics, Annual Review of Control, Robotics and Autonomous Systems, 2019, 2: 63–88.
23. N. Wang, Q. Deng, G. Xie, and X. Pan, Hybrid Finite-Time Trajectory Tracking Control of a Quadrotor, ISA Transactions, 2019, 90: 278–286.
24. D. Yang, Z. Li, P. Zhou, and J. Lu, Control System Design for Tiltable Quad-rotor with Propeller Failure, 2020 Chinese Automation Congress, pp:7473-7478, shanghai, China, November 6-8, 2020.
25. S. Zhang, Development of Unconventional Unmanned Aerial Vehicle With Tilt-Rotor Platform, PhD thesis of National University of Singapore, 2018.
26. N. Zhao, Y. Luo, H. Deng, and Y. Shen, The deformable quad-rotor: Design, Kinematics and Dynamics Characterization, and Flight Performance Validation, 2017 IEEE/RSJ International Conference on Intelligent Robots and Systems, Vancouver, BC, Canada, September 24-28, 2017.
27. P. Zheng, X. Tan, B. B. Kocer, E. Yang, and M. Kovac, TiltDrone: A Fully-Actuated Tilting Quadrotor Platform, IEEE Robotics and Automation Letters, 2020, 5(4): 6845–6852.
28. J. Lee, D. Lee, J. Kim, D. Kim, I. Jang, and H. J. Kim, Fully Actuated Autonomous Flight of Thruster-Tilting Multirotor, IEEE/ASME Transactions on Mechatronics, 2021, 26(2): 765–776.
29. A.M. Anaswamy, Adaptive Control and Intersections with Reinforcement Learning, Annual Review of Control, Robotics and Autonomous Systems, 2023, 6:65-93.
30. Z.T. Dydek, Adaptive Control of Unmanned Aerial Systems, PhD thesis of Massachusetts Institute of Technology, 2010.